New *G*-parity violating amplitude in the *J/ψ* decay?

R. Baldini Ferroli,[1] F. De Mori,[2,3] M. Destefanis,[2,3] M. Maggiora,[2,3] S. Pacetti,[4,*] L. Yan,[3,5] M. Bertani,[1] A. Calcaterra,[1] G. Felici,[1] P. Patteri,[1] Y. D. Wang,[1,6] A. Zallo,[1] D. Bettoni,[7] G. Cibinetto,[7] R. Farinelli,[7] E. Fioravanti,[7] I. Garzia,[7] G. Mezzadri,[7] V. Santoro,[7] M. Savrié,[8] F. Bianchi,[2] M. Greco,[2] S. Marcello,[2] S. Spataro,[2] C. M. Carloni Calame,[9] G. Montagna,[9,10] O. Nicrosini,[9] and F. Piccinini[9]

[1]*Laboratori Nazionali dell'INFN di Frascati, I-00044 Frascati, Italy*
[2]*Dipartimento di Fisica, Università di Torino, I-10125 Torino, Italy*
[3]*INFN Sezione di Torino, I-10125 Torino, Italy*
[4]*Dipartimento di Fisica e Geologia, Università degli Studi di Perugia and INFN Sezione di Perugia, I-06123 Perugia, Italy*
[5]*University of Science and Technology, Hefei 230026, People's Republic of China*
[6]*Helmholtz Institute, D-55099 Mainz, Germany*
[7]*INFN Sezione di Ferrara, I-44122 Ferrara, Italy*
[8]*Dipartimento di Fisica e Scienze della Terra, Università di Ferrara, I-44122 Ferrara, Italy*
[9]*INFN Sezione di Pavia, I-27100 Pavia, Italy*
[10]*Dipartimento di Fisica, Università di Pavia, Pavia, Italy*

The J/ψ meson has negative G parity so that, in the limit of isospin conservation, its decay into $\pi^+\pi^-$ should be purely electromagnetic. However, the measured branching fraction $\mathcal{B}(J/\psi \to \pi^+\pi^-)$ exceeds by more than 4.5 standard deviations the expectation computed according to *BABAR* data on the $e^+e^- \to \pi^+\pi^-$ cross section. The possibility that the two-gluon plus one-photon decay mechanism is not suppressed by G-parity conservation is discussed, even by considering other multipion decay channels. As also obtained by phenomenological computation, such a decay mechanism could be responsible for the observed discrepancy. Finally, we notice that the BESIII experiment, having the potential to perform an accurate measurement of the $e^+e^- \to \pi^+\pi^-$ cross section in the J/ψ mass energy region, can definitely prove or disprove this strong G-parity-violating mechanism by confirming or confuting the *BABAR* data.

I. INTRODUCTION

The J/ψ meson, like all the isoscalar vector mesons, having total angular momentum $J = 1$, negative C-parity, $C = -1$, and isospin zero, $I = 0$, possesses a well-defined G parity, i.e., $G = -1$. Indeed, particles that are eigenstates of the charge conjugation with eigenvalue C, are also eigenstates of G parity with eigenvalue $G = C(-1)^I$, where I is the isospin.

G parity is particularly useful because it is well defined also for those particles, which are not C-parity eigenstates, as those belonging to isospin multiplets, that have all the same value of G. Moreover, being a multiplicative quantum number, states containing particles eigenstates of G parity are themselves eigenstates of G parity with eigenvalue equal to the product of those of each particle. A state with n pions and no other particles has total G parity, $G_{n\pi} = (G_\pi)^n = (-1)^n$, since each pion, belonging to the same isospin multiplet, has the same G parity, i.e., $G_\pi = -1$.

The strong interaction conserves G parity, so that G is a good quantum number in QCD; on the contrary, the electromagnetic interaction can violate the isospin conservation and hence G parity.

II. *J/ψ* DECAY AMPLITUDES

The amplitude for the decay $J/\psi \to \mathcal{H}_q$, where $\mathcal{H}_q$ represents a final state containing only light hadrons, is usually parametrized as the sum of the three main contributions, $\mathcal{A}_{3g}$, $\mathcal{A}_{2g\gamma}$ and $\mathcal{A}_\gamma$, whose Feynman diagrams are shown in Fig. 1.

In general the amplitude $\mathcal{A}_\mathcal{I}$ describes the decay chain $J/\psi \to \mathcal{I} \to \mathcal{H}_q$, i.e., the J/ψ decay mediated by the virtual state $\mathcal{I}$ that could be three gluons, $\mathcal{I} = 3g$, two gluons plus one photon $\mathcal{I} = 2g + \gamma$, and a single photon, $\mathcal{I} = \gamma$. The branching fractions for these J/ψ decays, except for $\mathcal{I} = \gamma$, for which the one in the on-shell $\mu^+\mu^-$ final state is reported, are

$$\mathcal{B}(J/\psi \to 3g) = \frac{|\mathcal{A}_{3g}|^2 \cdot \mathrm{PS}_{3g}}{\Gamma_{J/\psi}}$$

$$= \frac{40(\pi^2 - 9)}{81\Gamma_{J/\psi}} \alpha_s^3(M_{J/\psi}) \frac{|\Psi(0)|^2}{m_c^2}$$

$$\times \left(1 + 4.9 \frac{\alpha_s(M_{J/\psi})}{\pi}\right), \qquad (1)$$

[*]simone.pacetti@pg.infn.it
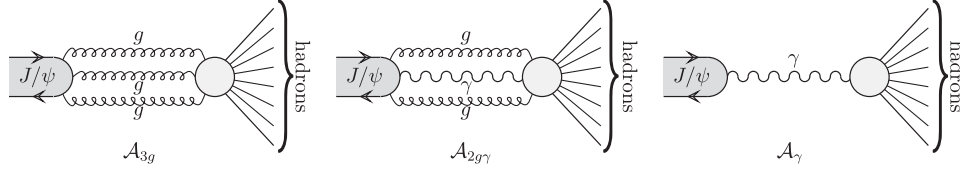
FIG. 1.   Feynman diagrams of the three main contributions to the amplitude of the decay $J/\psi \to$ hadrons.

$$\mathcal{B}(J/\psi \to 2g + \gamma) = \frac{|\mathcal{A}_{2g\gamma}|^2 \cdot \mathrm{PS}_{2g\gamma}}{\Gamma_{J/\psi}}$$

$$= \frac{128(\pi^2 - 9)}{81\Gamma_{J/\psi}} \alpha_s^2(M_{J/\psi})\alpha \frac{|\Psi(0)|^2}{m_c^2}$$

$$\times \left(1 - 0.9\frac{\alpha_s(M_{J/\psi})}{\pi}\right), \qquad (2)$$

$$\mathcal{B}(J/\psi \to \mu^+\mu^-) = \frac{|\mathcal{A}_\gamma J_{\mu^+\mu^-}|^2 \cdot \mathrm{PS}_{\mu^+\mu^-}}{\Gamma_{J/\psi}}$$

$$= \frac{64\pi}{9\Gamma_{J/\psi}} \alpha^2 \frac{|\Psi(0)|^2}{M_{J/\psi}^2}\left(1 - \frac{16}{3}\frac{\alpha_s(M_{J/\psi})}{\pi}\right),$$

$$(3)$$

where PS_f is the phase space for the final state f, m_c is the mass of the charm quark, $\Psi(r)$ is the $c\bar{c}$ wave function, and the quantities in parentheses are the first-order QCD corrections at the J/ψ mass. Equations (1) and (2) represent the branching fractions for the decays of the J/ψ into the intermediate states $3g$ and $2g + \gamma$ considered as on shell. The decay mode of Eq. (2) is usually considered negligible [1] with respect to the purely electromagnetic one of Eq. (3) and it has been ignored so far. This assumption is reconsidered later on. In Eq. (3) the amplitude $\mathcal{A}_\gamma$ is contracted with the pointlike electromagnetic current $J_{\mu^+\mu^-}$. The branching fraction $\mathcal{B}(J/\psi \to \mu^+\mu^-)$ can be related to that of the one-photon exchange decay of J/ψ into a hadronic final state, $\mathcal{H}_q$, $\mathcal{B}_\gamma(J/\psi \to \mathcal{H}_q)$, by considering the nonresonant dressed [2] cross section[1] at the J/ψ mass, as

---

[1]By dressed cross section we mean a cross section that includes the vacuum-polarization effects. The dressed Born cross section for the annihilation $e^+e^- \to \mathcal{H}_q$ is obtained by multiplying the corresponding bare cross section by $|\alpha(\sqrt{q^2})|^2/\alpha^2$, i.e.,

$$\sigma(e^+e^- \to \mathcal{H}_q)\left(\sqrt{q^2}\right) = \sigma^0(e^+e^- \to \mathcal{H}_q)(\sqrt{q^2})\frac{|\alpha(\sqrt{q^2})|^2}{\alpha^2},$$

where the superscript 0 stands for bare cross section, $\alpha = e^2/(4\pi) \simeq 1/137$ is the QED fine-structure constant, and $\alpha(\sqrt{q^2})$ is the QED running coupling constant, which includes vacuum-polarization effects.

$$\mathcal{B}_\gamma(J/\psi \to \mathcal{H}_q) = \mathcal{B}(J/\psi \to \mu^+\mu^-)$$

$$\times \frac{\sigma(e^+e^- \to \mathcal{H}_q)}{\sigma^0(e^+e^- \to \mu^+\mu^-)}\bigg|_{\sqrt{q^2}=M_{J/\psi}} \qquad (4)$$

where $\sigma^0(e^+e^- \to \mu^+\mu^-)$ stands for the bare (vacuum-polarization corrected) cross section.[2] The detailed derivation of Eq. (4) is reported in the Appendix. An upper limit can be obtained by considering all possible hadronic final states

$$\mathcal{B}_\gamma(J/\psi \to \mathcal{H}_q) < \mathcal{B}(J/\psi \to \mu^+\mu^-)\frac{|\alpha(M_{J/\psi})|^2}{\alpha^2}$$

$$\times \sum_{\mathcal{H}_q} \frac{\sigma(e^+e^- \to \mathcal{H}_q)}{\sigma^0(e^+e^- \to \mu^+\mu^-)}\bigg|_{\sqrt{q^2}=M_{J/\psi}}$$

$$= \mathcal{B}(J/\psi \to \mu^+\mu^-)R_{\mathrm{had}}(M_{J/\psi}), \qquad (5)$$

where R_{had} is the ratio of the bare or dressed nonresonant hadronic and muon cross sections in e^+e^- collisions and $\alpha(\sqrt{q^2})$ is the QED running coupling constant [3]. Such inequality is saturated once the sum over all possible hadronic final states for the J/ψ decay is considered, so that

$$\mathcal{B}_\gamma(J/\psi \to \mathrm{hadrons}) \equiv \sum_{\mathcal{H}_q} \mathcal{B}_\gamma(J/\psi \to \mathcal{H}_q)$$

$$= \mathcal{B}(J/\psi \to \mu^+\mu^-)R_{\mathrm{had}}(M_{J/\psi})$$

$$\times \frac{|\alpha(M_{J/\psi})|^2}{\alpha^2}$$

$$\simeq 2.63 \cdot \mathcal{B}(J/\psi \to \mu^+\mu^-).$$

The value 2.63 has been obtained by using the nonresonant values $R_{\mathrm{had}}(M_{J/\psi}) \simeq 2.5$ [4] and $|\alpha(M_{J/\psi})|^2/\alpha^2 \simeq 1.05$ [3,5]. In the case of a hadronic final state with negative G parity, as those containing only an odd number of pions, the strong amplitude $\mathcal{A}_{3g}$ is the dominant one. Moreover, by using the value $\alpha_s(M_{J/\psi}) = 0.135 \pm 0.015$, as extracted from the data on the ratio $\mathcal{B}(J/\psi \to 3g)/\mathcal{B}(J/\psi \to 2g + \gamma)$ [4] and Eqs. (1)–(3), we obtain the following ratios of branching ratios:
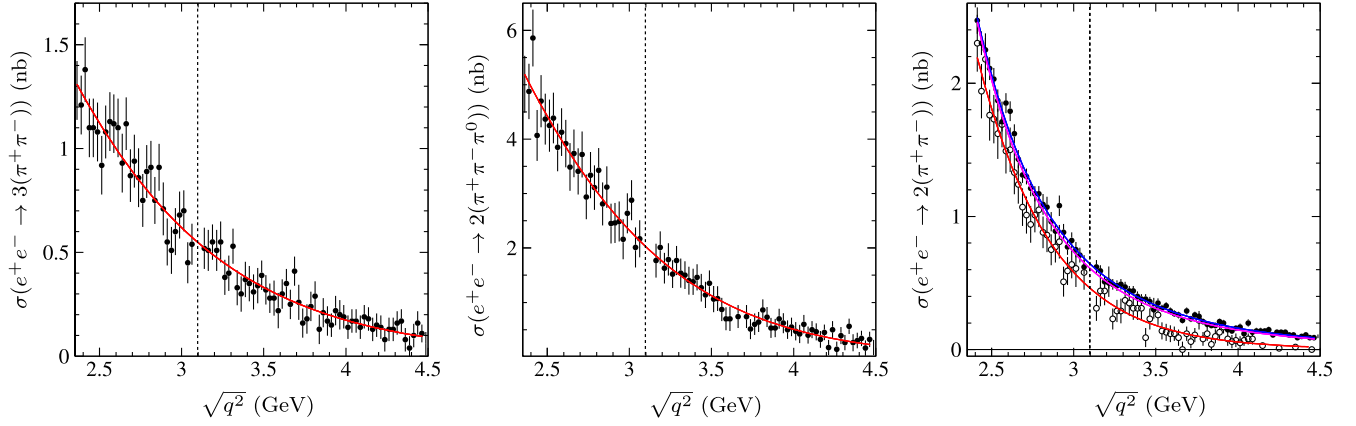
---

[2]See footnote 1.

FIG. 2.   Data and fit on the dressed cross sections: $3(\pi^+\pi^-)$ [6], left panel; $2(\pi^+\pi^-\pi^0)$ [6], central panel; $2(\pi^+\pi^-)$ from Ref. [7], empty circles; and Ref. [8], solid circles, right panel. The fits, shown as colored curves, have been performed in the region from $\sqrt{q^2} = 2.4$ GeV up to the highest $\sqrt{q^2}$ available data point, which, in all the cases, is at $\sqrt{q^2} \simeq 4.5$ GeV. In the four-pion case, right panel, two sets of data and three fits have been considered: 2012 data, blue, upper curve, 2005 data, red, lower curve, 2005 and 2012 data together, magenta, middle curve. The vertical dashed lines indicate the J/ψ mass.

$$\frac{\mathcal{B}(J/\psi \to 3g)}{\mathcal{B}(J/\psi \to 2g + \gamma)} = \frac{5}{16} \frac{\alpha_s(M_{J/\psi})}{\alpha} \frac{\pi + 4.9\alpha_s(M_{J/\psi})}{\pi - 0.9\alpha_s(M_{J/\psi})}$$

$$= 7.3 \pm 0.9,$$

$$\frac{\mathcal{B}(J/\psi \to 3g)}{\mathcal{B}(J/\psi \to \mu^+\mu^-)} = \frac{5(\pi^2 - 9)}{72\pi} \frac{M_{J/\psi}^2}{m_c^2} \frac{\alpha_s^3(M_{J/\psi})}{\alpha^2}$$

$$\times \frac{\pi + 4.9\alpha_s(M_{J/\psi})}{\pi - 16\alpha_s(M_{J/\psi})/3}$$

$$= 8 \pm 3. \tag{6}$$

Of particular interest are the decays of J/ψ into final states with positive G parity, $G = +1$, as for instance those consisting in an even number of pions. Indeed, since the strong interaction conserves G parity, the three-gluon contribution, $\mathcal{A}_{3g}$, is suppressed and such decays proceed mainly through the intermediate states γ and $2g + \gamma$ that, due to the presence of the photon, can violate the isospin conservation and hence G parity. Let us stress again that the $2g + \gamma$ contribution is considered negligible with respect to the single-photon one and is therefore ignored so far.

III. EVEN MULTIPION FINAL STATES

As already discussed in Sec. I, multipion final states, having well-defined G parity, represent useful and clean channels to test different models to parametrize the decay amplitudes and hence hypotheses about the dynamical mechanisms that rule the decay.

In particular, amplitudes of J/ψ decay into even numbers of pions; i.e., final states with $G = +1$ are assumed to be dominated by $\mathcal{A}_\gamma$, because G-parity conservation does not allow pure gluonic intermediate states.

Some G-parity-violation decay, not related to an electromagnetic contribution, has been observed, being interpreted as due to G-parity violation in the produced mesons, like in the case of $\rho - \omega$ or $f_0 - a_0$ mixing.

Figure 2 shows the nonresonant dressed cross section data and fits[3] in the $\sqrt{q^2} \geq 2.4$ GeV region, in case of $3(\pi^+\pi^-)$, $2(\pi^+\pi^-\pi^0)$ and $2(\pi^+\pi^-)$ [6] final states. To extract the nonresonant cross section values, reported in the first three rows of Table I, the data points lying in the J/ψ resonance region have been removed and hence not considered in the fitting procedures.

Concerning the $\pi^+\pi^-$ cross section, the only set of data that reaches $\sqrt{q^2} = 3$ GeV is the one collected by the *BABAR* experiment in 2006 [2], by means of the initial state radiation techniques (ISR). However, because of the large errors and the presence of structures nearby, the local fitting procedure, used in the previous cases, gives unreliable results. To avoid this limitation, the fitting procedure of Ref. [2] has been exploited. The fit function of the cross section, based on the Gounaris-Sakurai model [9] for the pion form factor, is shown in Fig. 3 superimposed to the data. Even though the *BABAR* data are on the bare cross section, the dressed value is recovered by using directly the pion form factor parametrization, which indeed is related to the dressed cross section. Moreover, since the Gounaris-Sakurai model does not embody the J/ψ contribution, the cross section value, extrapolated at $\sqrt{q^2} = M_{J/\psi}$, reported in Table I, is consequently not resonant. The one-photon

---

[3]Such a value has been obtained by fitting the cross section data in the energy range $\sqrt{q^2} \geq 2.4$ GeV, with the power law, $\sigma_{\text{fit}}(q^2; P_1, P_2, P_3) = P_1[(P_2^2 + M_{J/\psi}^2)/(P_2^2 + q^2)]^{P_3}$, where $P_1, P_2,$ and P_3 are free parameters. In particular, P_1 represents the cross section value at $\sqrt{q^2} = M_{J/\psi}$.

TABLE I. The dressed nonresonant cross section values (third column) have been obtained, as described in the text, by fitting or extrapolating the data, which are from Ref. [6] for the six pions, Ref. [7,8] for the four pions, and Ref. [2] for the two pions. The values of the last column are from Ref. [4]. The last row has been inserted to highlight a similar G-parity-violation phenomenon also for the $\psi(2S)$.

Decaying particle	$n\pi$ channel	$\sigma(e^+e^- \to 2n\pi)$ (nb) at $\sqrt{q^2} = M_{J/\psi}$	$\mathcal{B}_\gamma(J/\psi \to 2n\pi)$	$\mathcal{B}_{\mathrm{PDG}}(J/\psi \to 2n\pi)$
J/ψ	$3(\pi^+\pi^-)$	0.55 ± 0.02	$(3.62 \pm 0.12) \times 10^{-3}$	$(4.3 \pm 0.4) \times 10^{-3}$
	$2(\pi^+\pi^-\pi^0)$	2.03 ± 0.06	$(1.34 \pm 0.04) \times 10^{-2}$	$(1.62 \pm 0.21) \times 10^{-2}$
	$2(\pi^+\pi^-)$	0.612 ± 0.005	$(4.04 \pm 0.04) \times 10^{-3}$	$(3.57 \pm 0.30) \times 10^{-3}$
	$\pi^+\pi^-$	$(7.2 \pm 2.6) \times 10^{-3}$	$(4.7 \pm 1.7) \times 10^{-5}$	$(1.47 \pm 0.14) \times 10^{-4}$
$\psi(2S)$	$\pi^+\pi^-$	$\sigma(e^+e^- \to \pi^+\pi^-)$ (nb) extrapolated at $\sqrt{q^2} = M_{\psi(2S)}$ $(2.4 \pm 0.8) \times 10^{-3}$	$(3.0 \pm 1.0) \times 10^{-6}$	$(7.8 \pm 2.6) \times 10^{-6}$

amplitude appears as dominant, i.e., $\mathcal{B}_\gamma \simeq \mathcal{B}_{\mathrm{PDG}}$, in all the multipion J/ψ decays reported in Table I, with the exception of the $\pi^+\pi^-$ channel. Indeed, in this case, at most less than one-half of the observed rate can be explained by the contribution of $\mathcal{A}_\gamma$. The discrepancy exceeds 4.5 standard deviations.

If the discrepancy, observed by *BABAR*, is confirmed, an additional G-parity-violating decay amplitude should be considered. Such a further amplitude might strongly affect not only processes with branching ratios at the level of 10^{-4}, but also processes with branching ratios of the order of 10^{-3}, because of the interference among the amplitudes.

At least in the $\pi^+\pi^-$ case it might be that the one-photon amplitude does not dominate over the other G-parity-violating $2g + \gamma$ contribution; that indeed should be of the same order as $\mathcal{A}_\gamma$, not foreseen by previous estimates [10]. Unfortunately, it is quite difficult to compute such an

amplitude in the framework of QCD, even exploiting the formulas of Eqs. (1) and (2). Information about the relative strength of the $2g + \gamma$ amplitude with respect to the others might be inferred by considering odd-multipion decay channels, where G parity is conserved.

In the case of the four-pion channel, by assuming the one-photon dominance, the decay rate is overestimated by ~12% with respect to the PDG datum, even though the discrepancy is about one standard deviation. However, there exist two sets of data on the cross section $e^+e^- \to 2(\pi^+\pi^-)$; both of them have been collected by the *BABAR* experiment, the first in 2005 [7] with an integrated luminosity of 89 fb^{-1} and the second, in 2012 [8], with an integrated luminosity of 454.3 fb^{-1}. In the energy region around the J/ψ mass these two sets give different central values for the cross section. It is evident, see the right panel of Fig. 2, that the 2005 data (empty circles) are systematically below the more accurate 2012 data (solid circles). Table II reports cross sections and decay rates obtained by fitting these two sets separately (blue and red curves in the right panel of Fig. 2).

It is interesting to notice that only the result for $\mathcal{B}_\gamma$ based on the 2012 *BABAR* data exceeds the PDG value $\mathcal{B}_{\mathrm{PDG}}$. However, such a 20% discrepancy could be explained in terms of a constructive interference effect between a dominant $\mathcal{A}_\gamma$ and subdominant $\mathcal{A}_{2g\gamma} \simeq \mathcal{A}_\gamma/7$. New measurements of such a cross section in the J/ψ mass region would be of great value for establishing the actual strength of the electromagnetic amplitude.
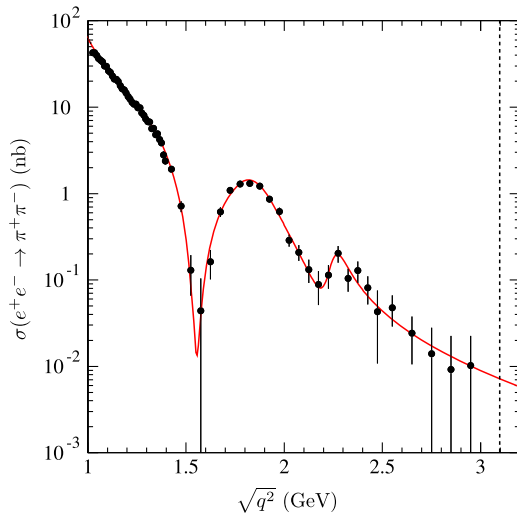

FIG. 3. Data and fit (red) on the $\pi^+\pi^-$ dressed nonresonant cross section [2]. The vertical dashed line indicates the J/ψ mass.

TABLE II. One-photon contributions to the decay rate of J/ψ into $2(\pi^+\pi^-)$ from 2005 and 2015 *BABAR* data.

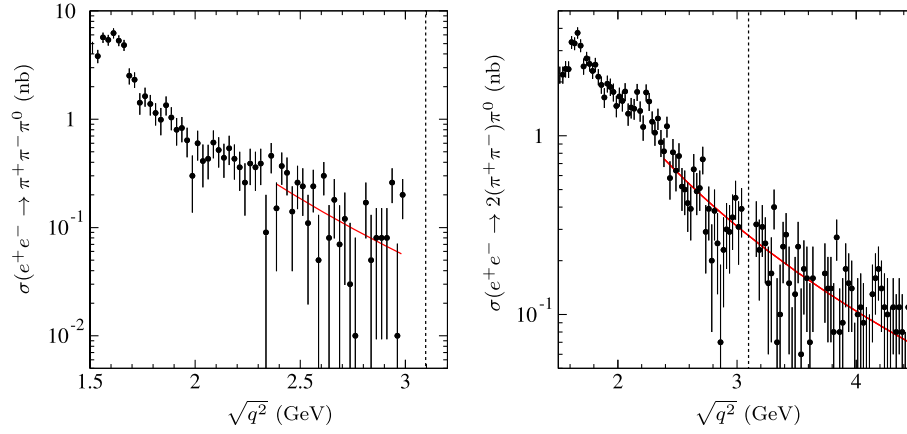| Year and reference	$\sigma(e^+e^- \to 2(\pi^+\pi^-))$ (nb) at $\sqrt{q^2} = M_{J/\psi}$	$\mathcal{B}_\gamma(J/\psi \to 2(\pi^+\pi^-))$
2005 [7]	0.463 ± 0.020	$(3.05 \pm 0.13) \times 10^{-3}$
2012 [8]	0.645 ± 0.006	$(4.24 \pm 0.05) \times 10^{-3}$

FIG. 4. The solid points represent the data on the $\pi^+\pi^-\pi^0$ [11] (left) and $2(\pi^+\pi^-)\pi^0$ [12] (right) cross section. The curves (red) are the fits, performed in the region $q^2 \geq 2.4$ GeV, and the vertical dashed lines indicate the J/ψ mass.

Finally, in the last row of Table I we also considered the $\psi(2S)$ decay into $\pi^+\pi^-$. To estimate the electromagnetic contribution, since there are no data, we extrapolate the $e^+e^- \to \pi^+\pi^-$ *BABAR* cross section at the $\psi(2S)$ mass, always by using the pion form factor parametrization of Ref. [2]. Even in the case as in that of the J/ψ, the electromagnetic contribution is responsible for less than the 40% of the measured branching fraction.

A. The *G*-parity-conserving channels

As a reference, the *G*-parity-conserving decays $J/\psi \to \pi^+\pi^-\pi^0$ and $J/\psi \to 2(\pi^+\pi^-)\pi^0$ are considered. The corresponding dressed production cross sections in e^+e^- annihilation have been measured by the *BABAR* experiment [11,12], again by means of the ISR, up to center of mass energies of $\sqrt{q^2} = 3$ and $\sqrt{q^2} = 4.5$ GeV, respectively. The values of such dressed nonresonant cross sections at $\sqrt{q^2} = M_{J/\psi}$, i.e.,

$$\sigma(e^+e^- \to \pi^+\pi^-\pi^0)(M_{J/\psi}) = 0.044 \pm 0.025 \text{ nb},$$
$$\sigma(e^+e^- \to 2(\pi^+\pi^-)\pi^0)(M_{J/\psi}) = 0.277 \pm 0.013 \text{ nb},$$

are obtained by means of the fitting procedure[4] used in Sec. III and shown in Fig. 4 together with the cross section data.

The electromagnetic decay rates can be computed by exploiting Eq. (4), as

$$\mathcal{B}_\gamma(J/\psi \to \pi^+\pi^-\pi^0)$$
$$= \mathcal{B}(J/\psi \to \mu^+\mu^-)\frac{\sigma(e^+e^- \to \pi^+\pi^-\pi^0)}{\sigma^0(e^+e^- \to \mu^+\mu^-)}\bigg|_{\sqrt{q^2}=M_{J/\psi}}$$
$$= (2.9 \pm 1.6) \times 10^{-4}, \tag{7}$$

---

[4] See footnote 3.

$$\mathcal{B}_\gamma(J/\psi \to 2(\pi^+\pi^-)\pi^0)$$
$$= \mathcal{B}(J/\psi \to \mu^+\mu^-)\frac{\sigma(e^+e^- \to 2(\pi^+\pi^-)\pi^0)}{\sigma^0(e^+e^- \to \mu^+\mu^-)}\bigg|_{\sqrt{q^2}=M_{J/\psi}}$$
$$= (1.82 \pm 0.08) \times 10^{-3}; \tag{8}$$

these values have to be compared with the PDG data

$$\mathcal{B}_{\text{PDG}}(J/\psi \to \pi^+\pi^-\pi^0) = (2.11 \pm 0.07) \times 10^{-2},$$
$$\mathcal{B}_{\text{PDG}}(J/\psi \to 2(\pi^+\pi^-)\pi^0) = (4.1 \pm 0.5) \times 10^{-2}.$$

Assuming that such decays are dominated by the three-gluon exchange mechanism, whose Feynman diagram is shown in the left panel of Fig. 1, the branching fractions can be parametrized following Eq. (1) as

$$\mathcal{B}_{3g}(J/\psi \to 3\pi, 5\pi)$$
$$= \mathcal{B}(J/\psi \to 3g)\left[\frac{4}{3}\alpha_s(M_{J/\psi})\right]^3 \cdot \text{PS}_{3\pi,5\pi}$$
$$= \frac{40(\pi^2-9)}{81\Gamma_{J/\psi}}\alpha_s^3(M_{J/\psi})\frac{|\Psi(0)|^2}{m_c^2}\left(1 + 4.9\frac{\alpha_s(M_{J/\psi})}{\pi}\right)$$
$$\times \left[\frac{4}{3}\alpha_s(M_{J/\psi})\right]^3 \cdot \text{PS}_{3\pi,5\pi},$$

where the factor $[4\alpha_s(M_{J/\psi})/3]^3$ accounts for the three-gluon vertices in the final state, while $\text{PS}_{3\pi(5\pi)}$ represents the three-pion (five-pion) phase space. In the same line of reasoning, the $2g + \gamma$ contributions, central panel of Fig. 1, are obtained from Eq. (2) as

TABLE III.   Cross sections and one-photon and two-gluon plus one-photon contributions to the branching fractions of the G-parity-conserving channels $\pi^+\pi^-\pi^0$ and $2(\pi^+\pi^-)\pi^0$, compared with the data from Ref. [4], reported in the last column.

$2(n+1)\pi$ channel	$\sigma(e^+e^- \to (2n+1)\pi)$ (nb) at $\sqrt{q^2} = M_{J/\psi}$	$\mathcal{B}_\gamma(J/\psi \to (2n+1)\pi)$	$\mathcal{B}_{2g\gamma}(J/\psi \to (2n+1)\pi)$	$\mathcal{B}_{\mathrm{PDG}}(J/\psi \to (2n+1)\pi)$
$\pi^+\pi^-\pi^0$	0.044 ± 0.025	$(2.9 \pm 1.6) \times 10^{-4}$	$(1.2 \pm 0.2) \times 10^{-4}$	$(2.11 \pm 0.07) \times 10^{-2}$
$2(\pi^+\pi^-)\pi^0$	0.277 ± 0.013	$(1.82 \pm 0.08) \times 10^{-3}$	$(2.3 \pm 0.3) \times 10^{-4}$	$(4.1 \pm 0.5) \times 10^{-2}$

$\mathcal{B}_{2g\gamma}(J/\psi \to 3\pi, 5\pi)$

$$= \mathcal{B}(J/\psi \to 2g + \gamma) \left[\frac{4}{3} \alpha_s(M_{J/\psi}) \right]^2 \alpha \cdot \mathrm{PS}_{3\pi,5\pi}$$

$$= \frac{128(\pi^2 - 9)}{81\Gamma_{J/\psi}} \alpha_s^2(M_{J/\psi}) \alpha \frac{|\Psi(0)|^2}{m_c^2} \left(1 - 0.9 \frac{\alpha_s(M_{J/\psi})}{\pi} \right)$$

$$\times \left[\frac{4}{3} \alpha_s(M_{J/\psi}) \right]^2 \alpha \cdot \mathrm{PS}_{3\pi,5\pi},$$

where, with respect to the previous case, there is only the exchange of a gluon propagator with a photon propagator; hence there are two powers of $\alpha_s(M_{J/\psi})$ and one of the electromagnetic coupling constant α, while the phase space is the same. Using the value $\alpha_s(M_{J/\psi}) = 0.135 \pm 0.015$ obtained in Sec. II, the first ratio of Eq. (6), and assuming that the PDG value is dominated by the three-gluon exchange contribution one gets

$$\mathcal{B}_{2g\gamma}(J/\psi \to \pi^+\pi^-\pi^0)$$
$$= \mathcal{B}_{\mathrm{PDG}}(J/\psi \to \pi^+\pi^-\pi^0)$$
$$\times \frac{\mathcal{B}(J/\psi \to 2g + \gamma)}{\mathcal{B}(J/\psi \to 3g)} \frac{\alpha}{4\alpha_s(M_{J/\psi})/3}$$
$$= (1.2 \pm 0.2) \times 10^{-4},$$
$$\mathcal{B}_{2g\gamma}(J/\psi \to 2(\pi^+\pi^-)\pi^0)$$
$$= \mathcal{B}_{\mathrm{PDG}}(J/\psi \to 2(\pi^+\pi^-)\pi^0)$$
$$\times \frac{\mathcal{B}(J/\psi \to 2g + \gamma)}{\mathcal{B}(J/\psi \to 3g)} \frac{\alpha}{4\alpha_s(M_{J/\psi})/3}$$
$$= (2.3 \pm 0.3) \times 10^{-4}.$$

Cross sections and branching fractions of the $\pi^+\pi^-\pi^0$ and $2(\pi^+\pi^-)\pi^0$ are summarized in Table III.

It is interesting to notice that, while the three-pion-$(2g + \gamma)$ rate is of the same order of $\mathcal{B}_\gamma(J/\psi \to \pi^+\pi^-\pi^0)$, given in Eq. (7), the five-pion-$(2g + \gamma)$ rate is 1 order of magnitude lower than the electromagnetic one, Eq. (8).

The different hierarchies among the contributions in these two channels and, in particular, the fact that $\mathcal{B}_\gamma$ and $\mathcal{B}_{2g\gamma}$ are of the same order in the case of $\pi^+\pi^-\pi^0$, while $\mathcal{B}_\gamma \gg \mathcal{B}_{2g\gamma}$ in the case of $2(\pi^+\pi^-)\pi^0$, are due to the values of the dressed nonresonant cross sections in e^+e^- annihilation. The cross section decreases with the pion multiplicity faster than the decay rate; indeed (at $\sqrt{q^2} = M_{J/\psi}$)

$$\frac{\sigma(e^+e^- \to \pi^+\pi^-\pi^0)}{\sigma(e^+e^- \to 2(\pi^+\pi^-)\pi^0)} \sim \frac{1}{6},$$
$$\frac{\mathcal{B}_{2g\gamma}(J/\psi \to \pi^+\pi^-\pi^0)}{\mathcal{B}_{2g\gamma}(J/\psi \to 2(\pi^+\pi^-)\pi^0)} = \frac{\mathcal{B}_{\mathrm{PDG}}(J/\psi \to \pi^+\pi^-\pi^0)}{\mathcal{B}_{\mathrm{PDG}}(J/\psi \to 2(\pi^+\pi^-)\pi^0)}$$
$$\sim \frac{1}{2}.$$

In other words, the drop of the e^+e^- cross section value as the pion multiplicity in the final state decreases makes the one-photon contribution comparable to the $2g + \gamma$ one. However, the dominance of the three-gluon amplitude in the G-parity-conserving channels hides this effect. On the contrary, in the G-parity-violating decays of the J/ψ, where the $\mathcal{A}_{3g}$ amplitude is suppressed, the effect of the drop of $\mathcal{B}_\gamma/\mathcal{B}_{2g\gamma}$ as the pion multiplicity decreases becomes important being that $\mathcal{A}_{2g\gamma}$ and $\mathcal{A}_\gamma$ are the dominant amplitudes.

In light of that, it is plausible that for the $\pi^+\pi^-$ final state, i.e., the multipion channel with the lowest multiplicity, the amplitudes $\mathcal{A}_{2g\gamma}$ and $\mathcal{A}_\gamma$ are similar and hence by considering $\mathcal{A}_\gamma$ only, as it has been done in Sec. III and shown in Table I, the decay rate is underestimated.

A computation of the $\mathcal{A}_{2g\gamma}$ contribution, made by means of a procedure based on a phenomenological description of the $2g + \gamma$ coupling, the Cutkosky rule [13], and the dispersion relations, has been made in Ref. [14]. By considering the only imaginary part of the amplitude $\mathcal{A}_{2g\gamma}$ and maximum interference with the one-photon amplitude it is obtained that

$$\mathcal{B}_{\gamma + \mathrm{Im}(2g+\gamma)}(J/\psi \to \pi^+\pi^-) = (10.8 \pm 2.7) \times 10^{-5}, \quad (9)$$

which is compatible with the PDG value of $\mathcal{B}_{\mathrm{PDG}}(J/\psi \to \pi^+\pi^-) = (14.7 \pm 1.4) \times 10^{-5}$.

IV. THE CLEO DATUM

Another unexpected result is represented by the high $e^+e^- \to \pi^+\pi^-$ cross section measured by the CLEO Collaboration [15] close to the $\psi(2S)$ mass, at $\sqrt{q^2} = 3.671$ GeV. The cross section value is

$$\sigma(e^+e^- \to \pi^+\pi^-)(M_{\psi(2S)}) = 9.0 \pm 2.3 \text{ pb}$$

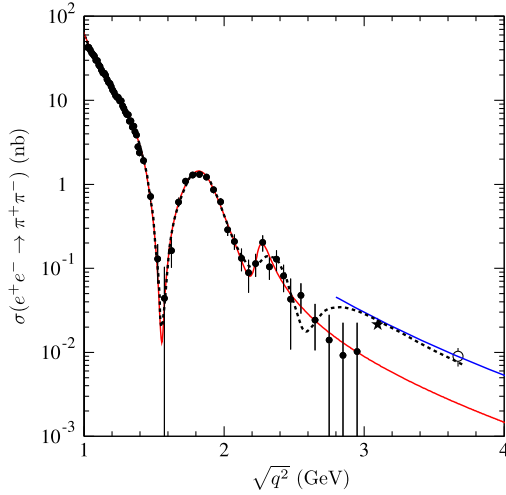and the corresponding data point is shown as an empty circle in Fig. 5.

FIG. 5.   The CLEO [15] datum (empty circle) together with *BABAR* [2] points (solid circles) and a theoretical estimate [16] of the $\pi^+\pi^-$ cross section at the J/ψ mass (solid star). The red curve is the fit on the *BABAR* data, the black dashed curve is the fit of Ref. [17], and the blue curve is cross section extrapolated from the CLEO point assuming the perturbative QCD power law [1].

This result is unexpected because, following perturbative QCD [1] (pQCD), at high $|q^2|$, the pion form factor should vanish with the power law $(q^2)^{-1}$; as a consequence, the cross section scales as

$$\sigma(e^+e^- \to \pi^+\pi^-)\left(\sqrt{q^2}\right)_{q^2\to\infty} \propto \left(\frac{1}{q^2}\right)^3.$$

Assuming the power-law behavior and relying on the only CLEO point, the nonresonant dressed cross section extrapolated at the J/ψ mass, blue curve in Fig. 5, is

$$\sigma(e^+e^- \to \pi^+\pi^-)(M_{J/\psi})_{\text{CLEO}} = (0.0251 \pm 0.0063) \text{ nb}.$$

This value is more than three times higher than that reported in Table I, obtained by the extrapolation of the *BABAR* data, red curve in Fig. 5; and, through the formula of Eq. (4), it gives the electromagnetic branching fraction

$$\mathcal{B}_\gamma^{\text{CLEO}}(J/\psi \to \pi^+\pi^-) = (1.65 \pm 0.42) \times 10^{-4},$$

which, being in agreement with the PDG value $\mathcal{B}_{\text{PDG}}(J/\psi \to \pi^+\pi^-) = (1.47 \pm 0.14) \times 10^{-4}$, confirms *G*-parity conservation, i.e., the one-photon-exchange dominance in the decay $J/\psi \to \pi^+\pi^-$.

However, as can be seen in Fig. 5, the two extrapolations, from *BABAR* data to higher $\sqrt{q^2}$ and from the CLEO point back to lower $\sqrt{q^2}$, are not compatible, that is, *BABAR* and CLEO data do not follow the pQCD behavior.

There are then three possibilities.

(i)   The *BABAR* measurement underestimates the cross section in the region 2.3–3.0 GeV by a factor of 3;

(ii) the CLEO datum overestimates the cross section at $\sqrt{q^2} = 3.671$ GeV by a factor of 3;

(iii) the high-$\sqrt{q^2}$ regime at which pQCD is expected to hold is still not reached, i.e., other prominent structures (strongly coupled high-mass resonances) are present and then *BABAR* and CLEO data are actually compatible.

The last possibility has been considered in Ref. [17], where the authors fit all the pion form factor data, including not only the CLEO point, but also a theoretical value [16] at the J/ψ mass, star symbol in Fig. 5, obtained from the branching ratio $\mathcal{B}_{\text{PDG}}(J/\psi \to \pi^+\pi^-)$, assuming *G*-parity conservation. The cross section obtained in Ref. [17] is shown as a black dashed curve in Fig. 5. The structure found at $\sqrt{q^2} \simeq 2.8$ GeV is due to the model used to fit the pion form factor data, which accounts not only for the "visible" resonances, but also for the infinite possible ρ radial excitations [18]. Nevertheless the last three *BABAR* points, with $\sqrt{q^2} \geq 2.7$ GeV, are hardly described.

V. THE WEIRD CASE OF $\omega\pi^0$

The decay $J/\psi \to \omega\pi^0$, with a branching fraction $\mathcal{B}_{\text{PDG}}(J/\psi \to \omega\pi^0) = (4.5 \pm 0.5) \times 10^{-4}$ [4], could be another channel where G parity is violated. Unfortunately there are no data on the cross section $\sigma(e^+e^- \to \omega\pi^0)$ at $\sqrt{q^2} = M_{J/\psi}$ that can be used to estimate, through Eq. (4), the electromagnetic contribution, $\mathcal{B}_\gamma(J/\psi \to \omega\pi^0)$. Nevertheless, data on such a cross section are available in other energy regions. In particular, as shown in Fig. 6, at low $\sqrt{q^2}$, the DM2 experiment [19] collected data in the range $(1.05 \leq \sqrt{q^2} \leq 2.00)$ GeV, while the SND experiment [20] covered the interval
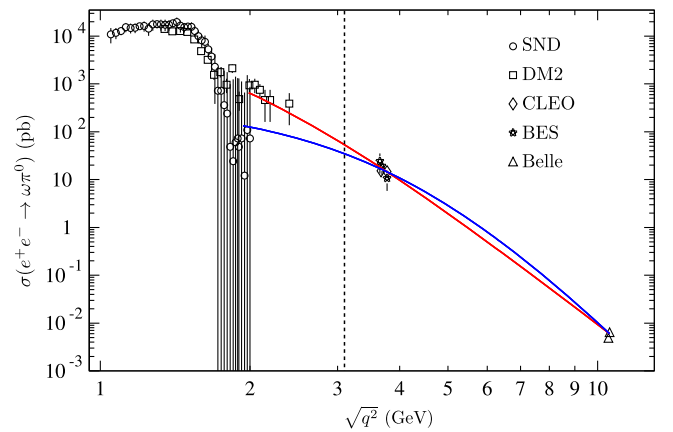

FIG. 6.   Data on the dressed nonresonant cross section $\sigma(e^+e^- \to \omega\pi^0)$ from SND [20] (empty circles), DM2 [19] (empty squares), BES [21] (empty stars), CLEO [22] (empty diamonds), and Belle [23] (empty triangles). The red and blue curves represent the fits described in the text, and the vertical dashed line indicates the J/ψ mass.

$(1.35 \le \sqrt{q^2} \le 2.40)$ GeV. Moreover, the cross section $\sigma(e^+e^- \to \omega\pi^0)$ has been measured around the $\psi(2S)$ and $\psi(3770)$ masses by the BES [21] and CLEO [22] experiments and in proximity of the $\Upsilon(4S)$ mass by the Belle experiment [23]. All the data, together with fits, are shown in Fig. 6. Following pQCD the expected asymptotic behavior for the cross section $\sigma(e^+e^- \to \omega\pi^0)$ as a function of q^2 is [1,24]

$$\sigma(e^+e^- \to \omega\pi^0)\left(\sqrt{q^2}\right) \underset{q^2 \to \infty}{\propto} |F_{\omega\pi^0}(q^2)|^2 \underset{q^2 \to \infty}{\propto} (q^2)^{-4}.$$

In light of this, to obtain the value at $\sqrt{q^2} = M_{J/\psi}$, the high energy data are fitted with[5]

$$\sigma_{\mathrm{asy}}(q^2; P_1, P_2, P_3) = P_1 \left(\frac{P_2^2 + M_{J/\psi}^2}{P_2^2 + q^2}\right)^{P_3},$$

where P_1, P_2, and P_3 are free parameters and P_1 represents the desired value of the cross section. Moreover, since the high energy tails of DM2 and SND data disagree, two fits have been performed by considering at low energy either the only DM2 data with $\sqrt{q^2} \ge 1.9$ GeV or the only SND data with $\sqrt{q^2} \ge 1.825$ GeV. These two lower limits have been chosen to have the same number of points from both DM2 and SND data sets. At higher energies, in both cases, all the available data from the BES, CLEO, and Belle experiments have been included. The two results, called DM2 and SND cases, are shown in Fig. 6 as curves (blue and red) superimposed to the data. The parameters and normalized χ^2's are reported in Table IV.

In the DM2 case, despite the large χ^2/d.o.f, the value of the P_3 parameter, which defines the power-law behavior, is in perfect agreement with the pQCD expectation that, on the contrary, is disregarded in the SND case. Finally, the electromagnetic contributions to the J/ψ branching fraction in the two cases are obtained by using the values of the P_1 parameter, which represents $\sigma(e^+e^- \to \omega\pi^0)(M_{J/\psi})$, in Eq. (4),

$$\mathcal{B}_\gamma(J/\psi \to \omega\pi^0)$$

$$= \mathcal{B}(J/\psi \to \mu^+\mu^-)\frac{\sigma(e^+e^- \to \omega\pi^0)}{\sigma^0(e^+e^- \to \mu^+\mu^-)}\bigg|_{\sqrt{q^2}=M_{J/\psi}}$$

$$= \begin{cases} (3.53 \pm 0.18) \times 10^{-4} & \text{DM2 case} \\ (2.29 \pm 0.40) \times 10^{-4} & \text{SND case} \end{cases},$$

to be compared with $\mathcal{B}_{\mathrm{PDG}}(J/\psi \to \omega\pi^0) = (4.5 \pm 0.5) \times 10^{-4}$.

---

[5]See footnote 3.

TABLE IV. Best parameters and normalized χ^2's for the fit function describing the $\omega\pi^0$ cross section.

Case	P_1 (pb)	P_2 (GeV)	P_3	χ^2/d.o.f.
DM2	53.6 ± 2.7	1.64 ± 0.21	4.07 ± 0.08	2.64
SND	34.8 ± 6.1	4.19 ± 0.08	5.55 ± 0.08	2.24

VI. AVAILABLE DATA SETS AND PROSPECTS FOR NEW MEASUREMENTS

The CLEO experiment [15] measured the $e^+e^- \to \pi^+\pi^-$ cross section at 3.671 GeV with about 20% statistical and 15% systematic accuracy, by collecting 20.7 pb^{-1}, corresponding to 26 candidate events. Pions have been identified mostly by means of the electromagnetic calorimeter. The most important background is due to the $\mu^+\mu^-$ channel; its contribution is estimated to be less than 10%.

The BESIII electromagnetic calorimeter and muon tracker [25] should provide similar, if not better performances. BESIII has collected 153 pb^{-1} at 3.08 GeV and 100 pb^{-1} at 2.9 GeV, which is more than ten times the luminosity collected by CLEO, from which the continuum cross section was obtained. Furthermore, the $\pi^+\pi^-$ cross section is larger close to the J/ψ mass with respect to the $\psi(2S)$ and the ratio $\sigma(e^+e^- \to \pi^+\pi^-)/\sigma^0(e^+e^- \to \mu^+\mu^-)$ is greater by a factor of $(M_{\psi(2S)}/M_{J/\psi})^4 \simeq 2$.

In the BESIII experiment, the pion identification at the ρ meson peak by means of ISR has been very successful [26], as shown in Fig. 7, where BESIII results are compared with the *BABAR* measurement [2]. Of course these results concern much higher $e^+e^- \to \pi^+\pi^-$ cross sections, quite lower pion energies, and different kinematical constraints, and this outstanding achievement cannot be directly applied to the studied case. However, even if not at such a high
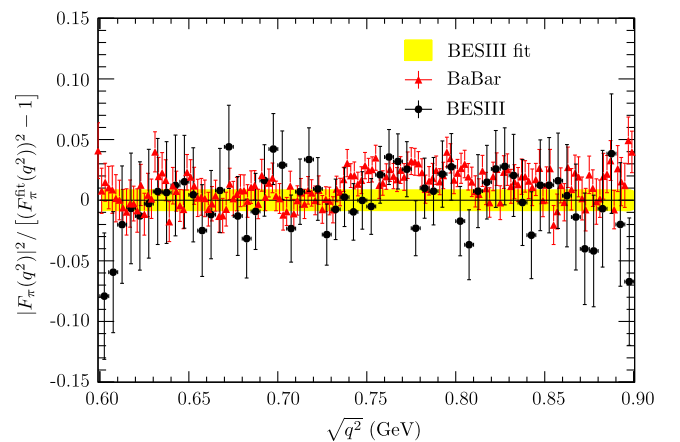

FIG. 7. Relative difference of the modulus squared of the pion form factor from *BABAR* [2] and the BESIII fit [26]; the figure is from Ref. [26]. Statistic and systematic uncertainties are included in the data points. The width of the BESIII band represents the systematic uncertainty only.

accuracy level, a precise measurement by BESIII, close to and at the J/ψ mass, can certainly be achieved.

VII. CONCLUSIONS

The *G*-parity-violating decay $J/\psi \to \pi^+\pi^-$ behaves differently with respect to the other J/ψ decays into even-multipion final states. There is a non-negligible disagreement, more than 4.5 standard deviations, between what is expected from the measurement of the dressed nonresonant cross section at the J/ψ mass and the measured branching ratio.

The J/ψ decay mechanism mediated by $2g + \gamma$, usually neglected, or better considered negligible being that it is *G*-parity violating, might be responsible for this discrepancy. Indeed, it happens that for this channel the one-photon contribution is so low that it might be of the same order of the $2g + \gamma$ one. The fact that the one-photon contribution becomes lower and lower as the pion multiplicity decreases has been shown in Table I, in the case of an even number of pions and in Table III in the case of an odd number of pions.

In Sec. III A, it has been noticed that, for the *G*-parity-conserving channels, the contribution to the branching fraction due to the $2g + \gamma$ intermediate state, which in this case can be estimated by exploiting its relation with the $3g$ contribution [Eqs. (1) and (2)], turns out to be comparable with $\mathcal{B}_\gamma$ especially in the case of the decay $J/\psi \to \pi^+\pi^-\pi^0$.

The phenomenological computation of $\mathcal{B}_{2g\gamma}(J/\psi \to \pi^+\pi^-)$ [14] corroborates the hypothesis about the softening and even the cancellation of the hierarchy between the two main contributions $\mathcal{B}_\gamma$ and $\mathcal{B}_{2g\gamma}$ in the case of lower multiplicity multipion final states. However, as a matter of fact, all the estimates, done until now, found the $2g + \gamma$ amplitude totally negligible with respect to the one-photon decay.

Finally, it has been shown that the BESIII experiment has the tools to repeat this measurement with high precision, to prove or disprove the discrepancy between $\mathcal{B}_\gamma(J/\psi \to \pi^+\pi^-)$ and $\mathcal{B}_{\mathrm{PDG}}(J/\psi \to \pi^+\pi^-)$ pointed out by the *BABAR* data.

If such a discrepancy is confirmed, the existence of this *G*-parity-violating amplitude can have heavy consequences for the attempts to get the relative phase between the strong and the electromagnetic J/ψ decay amplitudes, already in the case of branching ratios at the 10^{-3} level.

APPENDIX: THE MASTER FORMULA

The partial rate of the decay $J/\psi \to \gamma^* \to \mathcal{H}_q = \{h_1, …, h_n\}$, where the hadronic final state consists in a set of *n* hadrons h_j with 4-momenta p_j, $j = 1, …, n$, reads

$$d\Gamma_\gamma(J/\psi \to \mathcal{H}_q) = \frac{(2\pi)^4}{2M_{J/\psi}} \overline{|\mathcal{M}_\gamma(J/\psi \to \mathcal{H}_q)|^2} d\phi_n$$
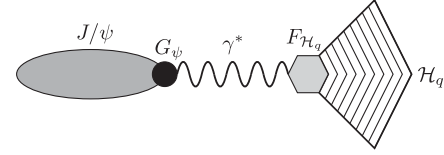$$\times (M_{J/\psi}; p_1, p_2, …, p_n),$$

FIG. 8. Feynman diagram of the decay $J/\psi \to \mathcal{H}_q$. The solid disc, the gray hexagon, and the lined area represent the J/ψ-γ coupling, the hadronic structure function, described in the text, and the hadronic final state, respectively.

where $\mathcal{M}_\gamma(J/\psi \to \mathcal{H}_q)$ is the Lorentz-invariant matrix element and $d\phi_n$ is an element of *n*-body phase space.

The Feynman diagram is shown in Fig. 8 and the matrix element is

$$\mathcal{M}_\gamma(J/\psi \to \mathcal{H}_q) = \epsilon^\mu(J/\psi) \frac{G_{J/\psi}}{q^2} H_\mu(p_j), \quad (A1)$$

where $\epsilon^\mu(J/\psi)$ is the J/ψ polarization vector, G_ψ is the J/ψ-γ coupling, $1/q^2$ is the photon propagator, and the Lorentz vector $H_\mu(p_j)$, depending on the 4-momenta of the final hadrons, describes the hadronic final state $\mathcal{H}_q$. The spin-averaged modulus squared of the matrix element given in Eq. (A1) is

$$\overline{|\mathcal{M}_\gamma(J/\psi \to \mathcal{H}_q)|^2}$$
$$= \frac{1}{3} \sum_{\mathrm{spins}} |\mathcal{M}_\gamma(J/\psi \to \mathcal{H}_q)|^2$$
$$= \frac{1}{3} \left(g^{\mu\nu} - \frac{P^\mu P^\nu}{M_{J/\psi}^2} \right) \frac{|G_{J/\psi}|^2}{(q^2)^2} \sum_{h\,\mathrm{spins}} H_\mu(p_j) H_\nu^\dagger(p_j)$$
$$\equiv \frac{1}{3} \left(g^{\mu\nu} - \frac{P^\mu P^\nu}{M_{J/\psi}^2} \right) \frac{|G_{J/\psi}|^2}{(q^2)^2} \mathcal{F}_{\mu\nu}(p_j), \quad (A2)$$

where P^μ is the J/ψ 4-momentum and the tensor $\mathcal{F}_{\mu\nu}(p_j)$ is defined as

$$\mathcal{F}_{\mu\nu}(p_j) \equiv \sum_{h\,\mathrm{spins}} H_\mu(p_j) H_\nu^\dagger(p_j).$$

As a consequence of the current conservation, $P^\alpha \mathcal{F}_{\alpha\mu} = P^\beta \mathcal{F}_{\mu\beta} = 0$, the tensor structure of $\mathcal{F}_{\mu\nu}(p_j)$ can be defined as

$$\mathcal{F}_{\mu\nu} = (g^{\mu\nu}P^2 - P^\mu P^\nu) F_{\mathcal{H}_q}(P^2; p_j), \quad (A3)$$

where $F_{\mathcal{H}_q}(P^2; p_j)$ is a Lorentz scalar structure function, depending on all the scalar quantities that can be obtained by using the 4-momenta and the Lorentz tensors related to the spin structure of the final hadrons (e.g., in case of a baryon-antibaryon final state, $\mathcal{H}_q = \{B, \bar{B}\}$, these Lorentz tensors are the Dirac gamma matrices). Using such a

definition and considering on-shell J/ψ mesons, with $q = P$ and $q^2 = P^2 = M^2_{J/\psi}$, the spin-averaged modulus squared of the matrix element of Eq. (A2) reads

$$\overline{|\mathcal{M}_\gamma(J/\psi \to \mathcal{H}_q)|^2} = \frac{|G_{J/\psi}|^2}{3M^4_{J/\psi}} 3P^2 F_{\mathcal{H}_q}(q^2, p_j)$$

$$= \frac{|G_{J/\psi}|^2}{M^2_{J/\psi}} F_{\mathcal{H}_q}(M^2_{J/\psi}, p_j),$$

and the partial decay rate becomes

$$d\Gamma_\gamma(J/\psi \to \mathcal{H}_q) = \frac{(2\pi)^4 |G_{J/\psi}|^2}{2M^3_{J/\psi}} F_{\mathcal{H}_q}(M^2_{J/\psi}, p_j) d\phi_n$$

$$\times (M_{J/\psi}; p_1, p_2, \ldots, p_n).$$

The total rate is obtained by integrating in $d\phi_n$, i.e.,

$$\Gamma_\gamma(J/\psi \to \mathcal{H}_q) = \frac{(2\pi)^4 |G_{J/\psi}|^2}{2M^3_{J/\psi}} \int F_{\mathcal{H}_q}(M^2_{J/\psi}, p_j)$$

$$\times d\phi_n(M_{J/\psi}; p_1, p_2, \ldots, p_n), \qquad (A4)$$

where the multiparticle structure is described by the function $F_{\mathcal{H}_q}(M^2_{J/\psi}, p_j)$.

The differential cross section for the annihilation process $e^+ e^- \to \gamma^* \to \mathcal{H}_q$ is

$$d\sigma(e^+ e^- \to \mathcal{H}_q) = \frac{(2\pi)^4 \overline{|\mathcal{M}(e^+ e^- \to \mathcal{H}_q)|^2}}{4\sqrt{(k_1 k_2)^2 - m_e^4}}$$

$$\times d\phi_n(k_1 + k_2; p_1, p_2, \ldots, p_n),$$

where $k^\mu_{1(2)}$ is the electron (positron) 4-momentum. In the $e^+ e^-$ center of mass frame and neglecting the electron mass, the previous expression reads

$$d\sigma(e^+ e^- \to \mathcal{H}_q) = \frac{(2\pi)^4 \overline{|\mathcal{M}(e^+ e^- \to \mathcal{H}_q)|^2}}{2q^2}$$

$$\times d\phi_n(q; p_1, p_2, \ldots, p_n),$$

with $q = k_1 + k_2$.

In Born approximation of the annihilation process is described by the Feynman diagram shown in Fig. 9, whose matrix element reads

$$\mathcal{M}(e^+ e^- \to \mathcal{H}_q) = i\bar{v}(k_2)\gamma^\mu u(k_1)\frac{e}{q^2} H_\mu(p_j),$$

where $u(k_1)$ and $v(k_2)$ are the electron and positron spinors. Using, for the contraction of the hadronic vectors, the expression of Eq. (A3), the spin-averaged modulus squared of the matrix element is
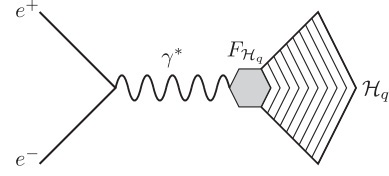

FIG. 9. Feynman diagram of the annihilation $e^+ e^- \to \mathcal{H}_q$ in Born approximation. The gray hexagon and the lined area represent the hadronic structure function and the hadronic final state, respectively.

$$\overline{|\mathcal{M}(e^+ e^- \to \mathcal{H}_q)|^2}$$

$$= \frac{1}{4} \sum_{\text{spins}} |\mathcal{M}(e^+ e^- \to \mathcal{H}_q)|^2$$

$$= -\left(k_1^\mu k_2^\nu + k_2^\mu k_1^\nu - \frac{q^2}{2}g^{\mu\nu}\right)\frac{e^2}{(q^2)^2}(g^{\mu\nu}q^2 - q^\mu q^\nu)$$

$$\times F_{\mathcal{H}_q}(q^2, p_j)$$

$$= (q^2)^2 \frac{e^2}{(q^2)^2} F_{\mathcal{H}_q}(q^2, p_j)$$

$$= 4\pi\alpha F_{\mathcal{H}_q}(q^2, p_j).$$

The differential and total cross sections are

$$d\sigma(e^+ e^- \to \mathcal{H}_q) = \frac{(2\pi)^4 4\pi\alpha}{2q^2} F_{\mathcal{H}_q}(q^2, p_j)$$

$$\times d\phi_n(q; p_1, p_2, \ldots, p_n),$$

$$\sigma(e^+ e^- \to \mathcal{H}_q)\left(\sqrt{q^2}\right) = \frac{(2\pi)^4 4\pi\alpha}{2q^2} \int F_{\mathcal{H}_q}(q^2, p_j)$$

$$\times d\phi_n(q; p_1, p_2, \ldots, p_n). \quad (A5)$$

By taking the ratio between total decay rate, Eq. (A4), and total cross section, Eq. (A5), at the J/ψ mass, the common phase-space integral cancels,

$$\frac{\Gamma_\gamma(J/\psi \to \mathcal{H}_q)}{\sigma(e^+ e^- \to \mathcal{H}_q)(M_{J/\psi})} = \frac{(2\pi)^4 |G_{J/\psi}|^2}{2M^3_{J/\psi}} \frac{2M^2_{J/\psi}}{(2\pi)^4 4\pi\alpha}$$

$$= \frac{|G_{J/\psi}|^2}{4\pi\alpha M_{J/\psi}}. \qquad (A6)$$

In order to obtain a relation among only measurable quantities, the value $|G_{J/\psi}|^2$, the modulus squared of the γ-J/ψ coupling has to be related to the rate of the purely decay $J/\psi \to \mu^+\mu^-$, whose Feynman diagram is shown in Fig. 10.

By neglecting the muon mass, being $m_\mu \ll M_{J/\psi}$, the rate is

$$\Gamma(J/\psi \to \mu^+\mu^-) = \frac{\alpha|G_{J/\psi}|^2}{3M_{J/\psi}^3}. \qquad (A7)$$

Using in Eq. (A6) the value $|G_{J/\psi}|^2$ extracted form Eq. (A7),

$$\frac{\Gamma_\gamma(J/\psi \to \mathcal{H}_q)}{\sigma(e^+e^- \to \mathcal{H}_q)(M_{J/\psi})} = \frac{3M_{J/\psi}^2}{4\pi\alpha^2}\Gamma(J/\psi \to \mu^+\mu^-)$$

$$= \frac{\Gamma(J/\psi \to \mu^+\mu^-)}{4\pi\alpha^2/(3M_{J/\psi}^2)}$$

$$= \frac{\Gamma(J/\psi \to \mu^+\mu^-)}{\sigma^0(e^+e^- \to \mu^+\mu^-)(M_{J/\psi})},$$

$$(A8)$$

where the $e^+e^- \to \mu^+\mu^-$ bare Born cross section has been used,

$$\sigma^0(e^+e^- \to \mu^+\mu^-)\left(\sqrt{q^2}\right) = \frac{4\pi\alpha^2}{3q^2}.$$

Neither the decay rate $\Gamma_\gamma(J/\psi \to \mathcal{H}_q)$ nor the total cross section $\sigma(e^+e^- \to \mathcal{H}_q)$ has been corrected by the
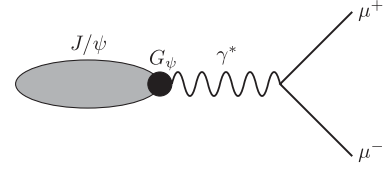

FIG. 10. Feynman diagram of the purely electromagnetic decay $J/\psi \to \mu^+\mu^-$. The solid disc represents the $J/\psi - \gamma^*$ coupling.

vacuum-polarization effects, so that they are dressed observables; indeed these effects are embodied in the hadronic vertex. It follows that the decay rate is defined in terms of the corresponding hadronic structure function $F_{\mathcal{H}_q}(q^2, p_j)$, evaluated at the J/ψ mass.

Finally, dividing Eq. (A8) by the J/ψ total width $\Gamma_{J/\psi}$, in order to have a relation between branching fractions, we obtain Eq. (4), i.e.,

$$\mathcal{B}_\gamma(J/\psi \to \mathcal{H}_q)$$

$$= \mathcal{B}(J/\psi \to \mu^+\mu^-)\frac{\sigma(e^+e^- \to \mathcal{H}_q)}{\sigma^0(e^+e^- \to \mu^+\mu^-)}\bigg|_{q^2=M_{J/\psi}^2}.$$

[1] V. L. Chernyak and A. R. Zhitnitsky, JETP Lett. **25**, 510 (1977); G. P. Lepage and S. J. Brodsky, Phys. Rev. D **22**, 2157 (1980); S. J. Brodsky and G. P. Lepage, Phys. Rev. D **24**, 2848 (1981); V. Chernyak, arXiv:hep-ph/9906387; V. L. Chernyak and A. R. Zhitnitsky, Phys. Rep. **112**, 173 (1984); V. V. Braguta, A. K. Likhoded, and A. V. Luchinsky, Phys. Rev. D **78**, 074032 (2008).

[2] J. P. Lees *et al.* (BABAR Collaboration), Phys. Rev. D **86**, 032013 (2012).

[3] F. Jegerlehner, Nuovo Cim. C **034S1**, 31 (2011).

[4] K. A. Olive *et al.* (Particle Data Group Collaboration), Chin. Phys. C **38**, 090001 (2014).

[5] F. Jegerlehner, http://www-com.physik.hu-berlin.de/~fjeger/.

[6] B. Aubert *et al.* (BABAR Collaboration), Phys. Rev. D **73**, 052003 (2006).

[7] B. Aubert *et al.* (BABAR Collaboration), Phys. Rev. D **71**, 052001 (2005).

[8] J. P. Lees *et al.* (BABAR Collaboration), Phys. Rev. D **85**, 112009 (2012).

[9] G. J. Gounaris and J. J. Sakurai, Phys. Rev. Lett. **21**, 244 (1968).

[10] V. L. Chernyak and A. R. Zhitnitsky, Nucl. Phys. **B201**, 492 (1982); **B214**, 547 (1983); Phys. Rep. **112**, 173 (1984).

[11] B. Aubert *et al.* (BABAR Collaboration), Phys. Rev. D **70**, 072004 (2004).

[12] B. Aubert *et al.* (BABAR Collaboration), Phys. Rev. D **76**, 092005 (2007); **77**, 119902 (2008).

[13] R. E. Cutkosky, J. Math. Phys. (N.Y.) **1**, 429 (1960).

[14] R. Baldini Ferroli, A. Mangoni, and S. Pacetti, arXiv: 1611.04437.

[15] T. K. Pedlar *et al.* (CLEO Collaboration), Phys. Rev. Lett. **95**, 261803 (2005).

[16] J. Milana, S. Nussinov, and M. G. Olsson, Phys. Rev. Lett. **71**, 2533 (1993).

[17] H. Czyz, A. Grzelinska, and J. H. Kuhn, Phys. Rev. D **81**, 094014 (2010).

[18] C. A. Dominguez, Phys. Lett. B **512**, 331 (2001).

[19] D. Bisello *et al.*, Nucl. Phys. B, Proc. Suppl. **21**, 111 (1991).

[20] M. N. Achasov, V. M. Aulchenko, A. Y. Barnyakov, K. I. Beloborodov, A. V. Berdyugin, A. G. Bogdanchikov, A. A. Botov, T. V. Dimova *et al.*, Phys. Rev. D **88**, 054013 (2013).

[21] M. Ablikim *et al.* (BES Collaboration), Phys. Rev. D **70**, 112007 (2004); **71**, 019901 (2005).

[22] G. S. Adams *et al.* (CLEO Collaboration), Phys. Rev. D **73**, 012002 (2006).

[23] C. P. Shen *et al.* (Belle Collaboration), Phys. Rev. D **88**, 052019 (2013).

[24] S. Pacetti, Eur. Phys. J. A **38**, 331 (2008).

[25] M. Ablikim *et al.* (BESIII Collaboration), Nucl. Instrum. Methods Phys. Res., Sect. A **614**, 345 (2010).

[26] M. Ablikim *et al.* (BESIII Collaboration), Phys. Lett. B **753**, 629 (2016).